Spatial Regulation of Inflammation by Human Aortic Endothelial Cells in a Linear Gradient of Shear Stress

JEAN K. TSOU,* R. MICHAEL GOWER,* HAROLD J. TING,* ULRICH Y. SCHAFF,* MICHAEL F. INSANA,† ANTHONY G. PASSERINI,* AND SCOTT I. SIMON*

*Department of Biomedical Engineering, University of California, Davis, California, USA

†Department of Bioengineering, University of Illinois, Urbana-Champaign, Illinois, USA

QUERY SHEET

Q1: Au: Please reorder references so that the in text citations appear consecutively in the manuscript.

Q2: Au: adherents meant?

informa
healthcare

Ensure the widest reach for your article and research!

Informa Reprints provides a valuable service to the pharmaceutical and medical device industries by alerting product and brand managers to key journal articles of therapeutic relevance and securing quantity distribution for educational purposes. If you feel your article would be of educational value to industry, please take a minute to fill out the form below and return it to our Reprints Dept. Thank you.

E-mail: journalreprints@informausa.com
Fax: (212) 520-2705
Mail: Informa Healthcare
Attn: Neil Adams, Reprints Department
52 Vanderbilt Avenue, 16th Floor
New York, NY 10017

Article Title: _____

Journal Title: _____ MS ID #: _____

Companies or organizations that may be interested in ordering reprints of your article:

Company: _____ **Product/Brand Manager Contact:** _____

Drug/Product Relevance:_____

Address: _____

City: _____ State: _____ Zip: _____

Phone number: _____ E-mail: _____

Company: _____ **Product/Brand Manager Contact:** _____

Drug/Product Relevance:_____

Address: _____

City: _____ State: _____ Zip: _____

Phone number: _____ E-mail: _____

Microcirculation, iFirst: 1–13, 2007

ISSN: 1073-9688 print / 1549-8719 online
DOI: 10.1080/10739680701724359

informa
healthcare

Spatial Regulation of Inflammation by Human Aortic Endothelial Cells in a Linear Gradient of Shear Stress

JEAN K. TSOU,* R. MICHAEL GOWER,* HAROLD J. TING,* ULRICH Y. SCHAFF,*
MICHAEL F. INSANA,† ANTHONY G. PASSERINI,* AND SCOTT I. SIMON*
*Department of Biomedical Engineering, University of California, Davis, California, USA
†Department of Bioengineering, University of Illinois, Urbana-Champaign, Illinois, USA

ABSTRACT

Objective: Atherosclerosis is a focal disease that develops at sites of low and oscillatory shear stress in arteries. This study aimed to understand how endothelial cells sense a gradient of fluid shear stress and transduce signals that regulate membrane expression of cell adhesion molecules and monocyte recruitment. **Methods:** Human aortic endothelial cells were stimulated with TNF-α and simultaneously exposed to a linear gradient of shear stress that increased from 0 to 16 dyne/cm^2. Cell adhesion molecule expression and activation of NFκB were quantified by immunofluorescence microscopy with resolution at the level of a single endothelial cell. Monocyte recruitment was imaged using custom microfluidic flow chambers. **Results:** VCAM-1 and E-selectin upregulation was greatest between 2–4 dyne/cm^2 (6 and 4-fold, respectively) and above 8 dyne/cm^2 expression was suppressed below that of untreated endothelial cells. In contrast, ICAM-1 expression and NFκB nuclear translocation increased with shear stress up to a maximum at 9 dyne/cm^2. Monocyte recruitment was most efficient in regions where E-selectin and VCAM-1 expression was greatest. **Conclusions:** We found that the endothelium can sense a change in shear stress on the order of 0.25 dyne/cm^2 over a length of ~10 cells, regulating the level of protein transcription, cellular adhesion molecule expression, and leukocyte recruitment during inflammation.
Microcirculation (2007) **iFirst,** 1–13. doi:10.1080/10739680701724359

KEY WORDS: atherosclerosis, inflammation, shear stress gradient, endothelium, monocyte

INTRODUCTION

Atherosclerosis is an inflammatory disease of arteries that occurs preferentially within characteristic geometries, such as curvatures and bifurcations, which correlate with disturbed flow characteristics, notably low time average shear stress (SS) and non-uniform gradients of SS [12, 25]. Shear stress imparted by the viscous flow of blood plays a significant role in the homeostasis of vascular structure and function in part through the action of the mechanically-responsive endothelium. Endothelial cell (EC) phenotypic heterogeneity is observed over spatial scales on the order of millimeters *in vivo* where disturbed flow profiles can result in an enhanced inflammatory response [30].

A hallmark of atherogenesis is the upregulation of endothelial cell adhesion molecules (CAMs) and concomitant recruitment of monocytes [31]. Promoting upregulation of CAMs are cytokines such as tumor necrosis factor-alpha (TNF-α) that elicit expression of intravascular cell adhesion molecule-1 (ICAM-1), vascular cell adhesion molecule-1 (VCAM-1), and E-selectin [1, 5, 6, 23]. The extent of monocyte recruitment is tightly regulated by the level of cytokine stimulation and the magnitude of fluid SS [36, 47]. The underlying mechanisms are not well understood since the magnitude of SS varies within vascular sites of disturbed flow where spatial gradients exist. For instance, regions of low SS and large spatial gradients exhibit amplified upregulation of VCAM-1 and E-selectin, which in turn increase monocyte capture even at a low concentration of cytokine stimulation [26]. Studies in which the SS is varied in order to

We would like to thank Dr. Sunichi Usami for his contribution of the original Hele-Shaw channel. This work is supported by NIH R01 AI47294 to SIS and NCI R01 CA082497 to MFI.

Address correspondance to Dr. Scott I. Simon, Department of Biomedical Engineering, University of California, Davis, 451 E. Health Sciences Dr., Genome and Biomedical Sciences Facility, Davis, CA 95616-5294. E-mail: sisimon@ucdavis.edu

correlate the inflammatory response have generally been performed at a constant magnitude. Elevated levels of SS as observed in arteries of healthy human subjects (i.e., 12–17 dyne/cm^2) are shown to be atheroprotective [13]. This has been in part attributed to attenuation of VCAM-1, despite the fact that ICAM-1 expression is upregulated at high SS. Conversely, preconditioning EC at low SS (i.e., 2–4 dyne/cm^2) as associated with regions of flow disturbance, results in pro-atherogenic conditions. These include membrane upregulation of VCAM-1 and E-selectin and increased efficiency of monocyte recruitment on inflamed EC [10, 15, 25, 26]. Thus, differential regulation of CAM transcription could result in changes that are both pro- and anti-inflammatory in the context of leukocyte recruitment [5, 6, 38, 40]. Spatial heterogeneity in the phenotype of EC *in vitro* as reported by Chen et al. [4] and White et al. [45] has been attributed to changes in shear direction or magnitude within a step flow chamber. Currently, there is a lack of information on the fundamental issue: how is CAM transcription/expression and concomitant leukocyte recruitment regulated on inflamed endothelium along a continuously varying SS field? Previous studies have not investigated with sufficient spatial resolution how EC function is regulated in response to SS and inflammation. Since atherosclerosis is a focal disease that typically develops in a steep SS gradient, a detailed study of how CAM expression and monocyte recruitment maps on inflamed EC is needed.

Studies performed in conventional parallel-plate flow chambers (PPFC) typically assay the response to a constant magnitude of SS over the length of the chamber by infusion at a defined flow rate. A range of SS is achieved by varying the flow rate in separate experiments [5, 6, 26, 40]. Here, we employed soft lithography techniques to create a modified version of a PPFC that delivers a linear decrease in SS from the inflow to the outflow. This made it possible to study EC function within a single chamber over a physiological range of SS with high spatial resolution while maintaining a constant shear gradient [43]. This chamber was applied to determine the relative importance of the magnitude versus the rate of change of SS as EC respond to TNF-α stimulation. We measured activation of NFκB and membrane upregulation of vascular CAMs (ICAM-1, VCAM-1 and E-selectin) and leukocyte recruitment efficiency to human aortic endothelium (HAEC) over a linear gradient of SS.

MATERIALS AND METHODS

Microfluidic Flow System: Linear Shear Stress Flow Chamber

The design of the flow chamber was adapted from Usami et al. based on Hele-Shaw flow theory [43]. A linear decrease in SS magnitude along the centerline of the channel, parallel to the longitudinal axis, was achieved by designing the sidewalls of the flow chamber to coincide with the streamlines of a two dimensional stagnation flow and making the end of the channel shaped to match the iso-potential lines (Fig. 1a). The channel width (w) is a function of axial distance (x), and it becomes wider toward the flow outlet:

$w = w_1 \frac{L}{L-x}$, where w_1 is the entrance width, L is the total length of the channel, x is the distance measured from the channel entrance. The generated wall SS (τ_w) along the center line is then described as:

$$\tau_w = \frac{6\mu\ Q}{h^2 w_1}\left(1 - \frac{x}{L}\right), \qquad (1)$$

where Q is the volumetric flow rate, μ is the viscosity of the flow medium, and h is the height of the channel. The dimension of the flow chamber used in this

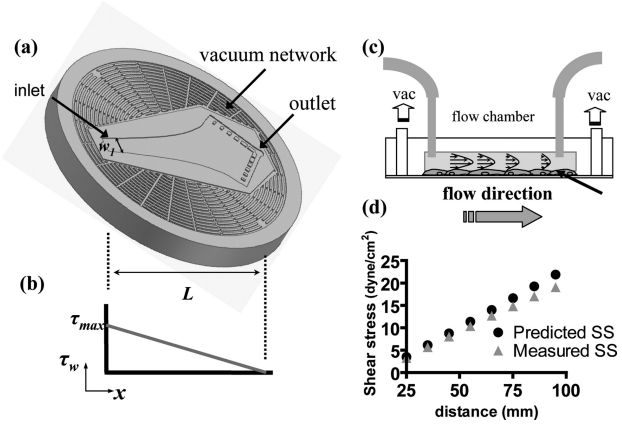

Figure 1. *Hele-Shaw linear shear stress gradient parallel plate flow chamber.* (a) PDMS mold of the linear shear flow chamber and surrounding vacuum network that seals the chamber to the HAEC monolayer on a cover slip. (b) Shear stress decreases linearly from entry to exit. (c) Flow chamber assembled over the HAEC monolayer. (d) Ultrasonic flow imaging measurements on a scaled-up version of the flow chamber with a w_1/L ratio of 3 mm/150 mm reveal a close correlation between the measured and estimated shear stress values ($R^2 = 0.99$).

study consists of the following parameters: $h = 100$ μm, $w_1 = 2$ mm, $L = 20$ mm. The linearity of SS with distance down the flow chamber, as defined by Equation 2 and depicted in Fig. 1b, was previously validated experimentally based on streamline analysis by Usami, et al [43]. In a companion study, we applied an ultrasonic flow imaging technique on a scaled-up model of the flow chamber with a w_1/L ratio of 3 mm/150 mm. As expected, the wall SS along the short axis is constant due to the symmetry of the flow profile at the cross sectional plane of the flow chamber. A high degree of correlation ($R^2 = .99$) was observed between the measured and computed SS values as plotted in Fig. 1d. The negative bias in ultrasound measurements is attributed to the spatial resolution of the ultrasound technique [39].

The design of the flow device consists of two major components: (I) the linear SS flow chamber and (II) the vacuum channel network. As shown in Fig. 1a, the spider web-like pattern is a network of vacuum channels that serves to seal the flow chamber to the cell-seeded cover slip surface in an aqueous environment in the absence of adhesives. The pattern on a silicon wafer was created using soft lithography and then served as a master for fabricating polydimethylsiloxane (PDMS) molds. The PDMS flow chamber is transparent and can be placed under a microscope for real time monitoring of the flow experiment, as recently described in detail [34].

Shear Flow Experiments

Primary HAEC isolated from a 16 year old Caucasian female (Cascade Biologics, Portland, Oregon, USA) at passage 6–7 were seeded on glass cover slips coated with 1% gelatin (Sigma-Aldrich, St. Louis, Missouri, USA) and grown to confluence in static culture within 3 days. The flow chamber was then placed and sealed onto the HAEC monolayer as described previously (Fig. 1c). HAEC were exposed to fluid SS ranging from 0 to 16 dyne/cm^2 for 4 hours, an interval previously shown to exert a prominent shear effect on CAM expression [6]. The nature of spatial variation in the shear field was such that EC over a length of 125 μm were exposed to a $\sim$0.1 dyne/cm^2 drop in SS.

Fluid flow was driven by a syringe pump (Harvard Apparatus, Holliston, Massachusetts, USA) operated in infuse mode. In order to stimulate the inflammatory response in selected experiments, TNF-α (R&D, Minneapolis, Minnesota, USA) at the concentration of 0.3 ng/mLwas delivered to the HAEC in the flow medium. Leibovitz-15 medium (GIBCO, Grand Island, New York, USA) mixed with 0.2% fetal bovine serum (Cascade Biologics) was used as the flow medium so that the pH could be properly maintained in the absence of CO_2 supply. Fifteen percent (wt/v) Ficoll PM 70 (Amersham biosciences, Piscataway, New Jersey, USA) was added to the flow medium to increase the viscosity to 3.26 ± 0.14 cp at 37°C , which approximates the viscosity of blood (3.2 cp) in large arteries [33]. Notably, the use of Ficoll at this concentration in previous studies did not affect leukocyte function, including the adhesiveness to unstimulated EC [14]. Flow rates of 0.1 and 0.07 mL/min were used to generate two different spatial SS gradients that differed in steepness by $\sim$30%.

Immunofluorescence Microscopy

For microscopic visualization of cell surface-associated proteins *in situ*, cells were incubated with fluorescently-labeled monoclonal antibodies (mAb) and followed by a secondary labeling using Qdot 605 (Quantum Dot, Hayward, California, USA) to provide a better image contrast. HAEC monolayers were then fixed in 2% paraformaldehyde (Sigma-Aldrich). The quantitative mean fluorescence intensity (MFI) from each field of view (250×250 μm) was captured via immunofluorescence microscopy and estimated using Image-Pro Plus (Media Cybernetics, Bethesda, Maryland, USA). This MFI was then used to compare shear-mediated CAM expression.

Detection of NFκB Nuclear Translocation

For microscopic visualization of nuclear phospho-p65, HAEC were exposed to a linear gradient of SS ranging from 0 to 16 dyne/cm^2 for 60 minutes while TNF-α at 1 ng/mL was delivered in the flow medium. Immediately following treatment, the flow chamber was removed from the glass cover slip, and the cell monolayer was then fixed and permeabilized with 1% paraformaldhyde and 40 μg/mL lysophosphatidylcholine (LPC) (Sigma-Aldrich) for 15 minutes at 4°C. Following fixation, the monolayer was incubated in 2.5% human serum albumin (Gemini, Sacramento, California, USA) for 15 minutes at 25°C to block non-specific binding. In order to image the onset of inflammatory activation, monolayers were incubated with 4 μg/mL anti-phospho-NFκB p65 (Cell Signaling, Danvers, Massachusetts, USA) for 1 hour at 25°C. Following

primary antibody treatment, monolayers were incubated with 50 μg/mL R-phycoerythrin goat anti-mouse IgG (Martek, Columbia, Maryland, USA) for 1 hour at 25°C. The cover slip was then sealed to a glass slide, and fluorescent images were then taken of the monolayer. Three representative 400 × 400 μm fields (containing 60–80 cells each) from five representative SS magnitudes were sampled, and the MFI of each nucleus was estimated using Image-Pro Plus. The threshold MFI for cell activation was set to a value such that only 15% of the non-TNF-α treated HAEC under static conditions were considered activated.

Leukocyte Isolation and Recruitment Assay

Heparin-anticoagulated whole blood was collected via a protocol approved by an internal review committee from healthy volunteers who gave informed consent. Neutrophils and monocytes were isolated using sedimentation over Lymphosep density separation medium (MP, Aurora, Ohio, USA) as previous described [2]. Monocytes were further purified using a negative isolation method with magnet beads (Dynal, Brown Deer, Wisconsin, USA). The final working concentration was controlled at 10^6 leukocytes/mL.

In order to observe the effects of SS and inflammatory stimulus on leukocyte recruitment efficiency, leukocytes perfused over pre-sheared EC at a constant flow rate. To accomplish this, two additional PDMS molds that consisted of three separate PPFC (width 300 μm [w_p] × depth 100 μm [h_p]) were fabricated to create uniform shear fields. In the first set of experiments, the original linear shear flow chamber was removed after 4 hours of shearing. The PPFCs were placed perpendicular to the original flow direction, such that they corresponded to lateral cross-sections of constant SS magnitude in the original chamber. Thus, leukocyte recruitment assays on regions of HAEC pre-sheared at defined magnitude was performed independently (Fig. 6a). We also considered the possible influence of spatial heterogeneity in shear-mediated CAM expression on EC-leukocyte interactions. Therefore, the PPFCs used in the second set of experiments were aligned parallel to the original shearing direction (Fig. 7a). The resulting SS when a leukocyte flows though the flow channel can be estimated via:

$$\tau_w = \frac{6\mu_L Q_L}{w_p h_p^2}.$$

The viscosity of the leukocyte solution $\mu_L$was approximately to that of water (1 cp), and with an input flow rate Q_L of 6 μL/min, it generated a shear field of 2 dyne/cm^2. For each flow channel, 5 image sequences (1 minute each) were recorded at a refresh rate of 2 frames per second. The images were manually analyzed offline.

Statistical Analysis

Analyses of the data were performed using GraphPad Prism version 4.0 software (GraphPad Software Inc, San Diego, California, USA). All data are reported as mean ± SEM, from 3 to 6 independent experiments as indicated. Data were analyzed by repeated measures ANOVA and secondary analysis for significance defined as $p < 0.05$ with Newman-Keuls post tests.

RESULTS

Endothelial CAM expression was measured as a function of distance down the flow channel, in which SS decreased linearly from 16 dyne/cm^2 at the inlet to essentially zero at the exit (Fig. 2). This SS range was chosen to model the transition from atheroprotective (i.e., $\geq$12 dyne/cm^2) to athero-prone (i.e., $\leq$4 dyne/cm^2) arterial regions as defined in previous studies [25]. Representative images of ICAM-1, VCAM-1 and E-selectin immunofluorescence depicted in Fig. 2 correspond to distances 3, 6, 12 and 18 mm downstream of the chamber inlet. Elongation or realignment of HAEC over the 4 hour duration of SS was not apparent. CAM expression after 4 hours of TNF-α in the presence of laminar SS was quantified by image analysis over distinct ~1 mm^2 regions, corresponding to an area on the monolayer containing ~50 HAEC. The relative change in CAM expression as a function of the magnitude of SS over discrete areas is plotted in Fig. 3 as the percent of unstimulated EC MFI under static conditions. Addition of TNF-α (0.3 ng/mL) under static conditions stimulated upregulation of VCAM-1 by ~350%, and ICAM-1 and E-selectin by 150% and 250%, respectively. Shear alone elicited a 100% increase in ICAM-1 expression at high SS, whereas VCAM-1 and E-selectin expression was not significantly upregulated at any position along the gradient.

In the presence of SS and TNF-α, ICAM-1 expression increased linearly with SS rising to 450% of the unstimulated static condition, before reaching a plateau at ~9 dyne/cm^2(Fig. 3a). VCAM-1 and E-selectin exhibited a very different response in that maximal

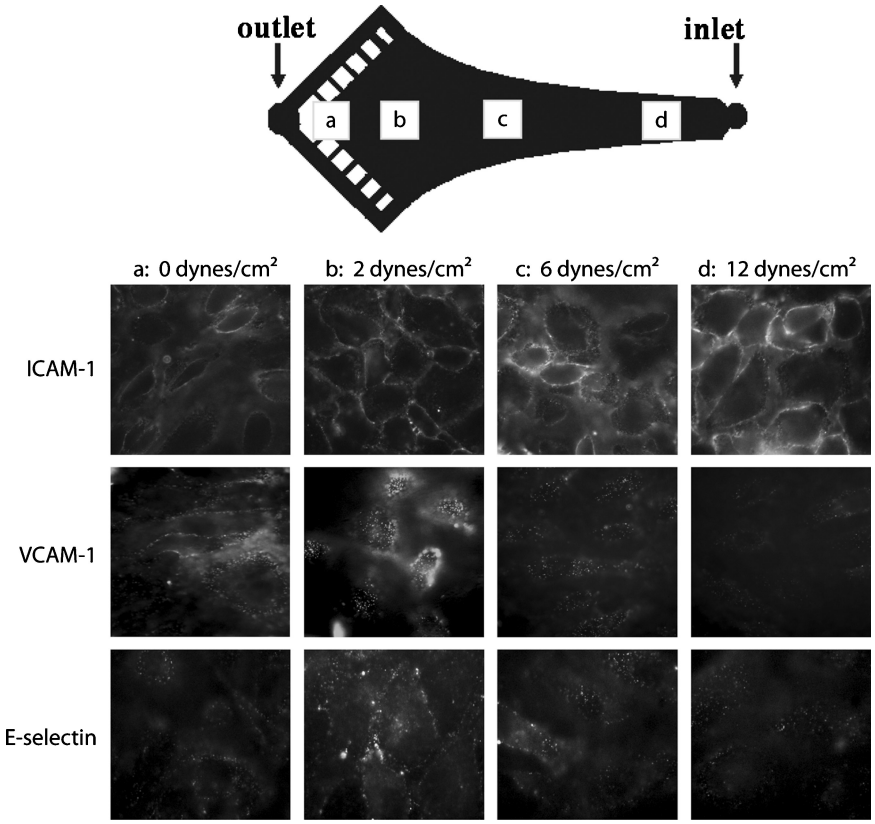

Figure 2. *Representative immunofluorescence images of cell adhesion molecule (ICAM-1, VCAM-1, and E-selectin)* surface expression down a linear shear field. Images are oriented parallel to the flow stream lines and are sampled from regions as indicated in the schematic: (a) 0 (b) 2 (c) 6 and (d) 12 dyne/cm^2.

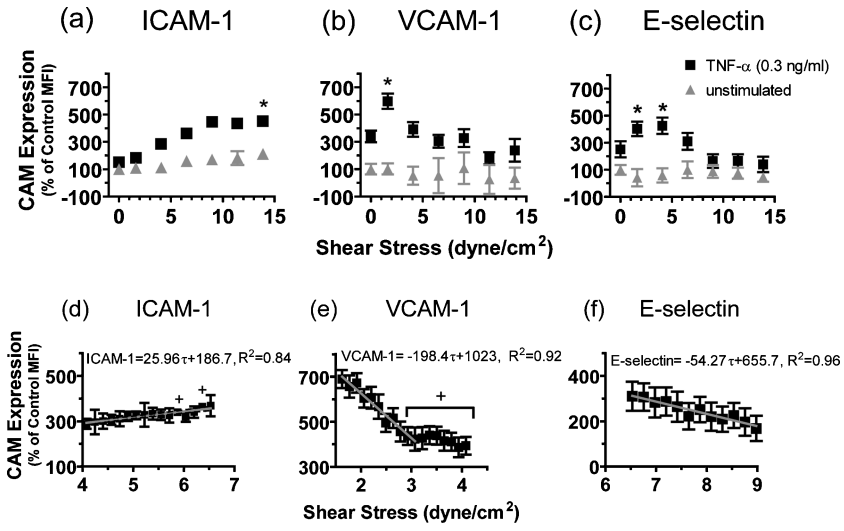

Figure 3. *CAM expression as a function of shear stress down the Hele-Shaw chamber.* (a) ICAM-1, (b) VCAM-1 and (c) E-selectin. (d)-(f) The corresponding CAM expression acquired at higher magnification over the indicated shear stress regimes. Data are presented as percentage of unstimulated static control EC MFI and shown as mean ± SEM from 3 to 6 independent experiments. * $p < 0.05$ versus TNF-α stimulated static ECs. + $p < 0.05$ versus the condition exposed to the lowest shear stress shown in the plots.

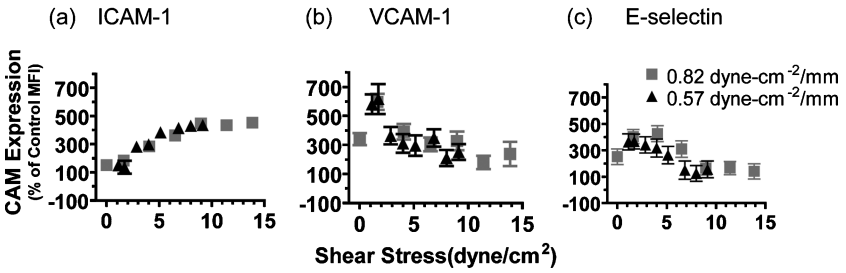

Figure 4. *Spatial CAM regulation is dependent on the magnitude and not gradient of applied shear stress*. Two distinct spatial shear gradients 0.82 and 0.57 dyne/cm^2 per mm were applied. Varying spatial gradients in shear stress shows no significant alteration in CAM expression. Data are presented as percentage of unstimulated static control EC MFI and shown as mean ± SEM from 3 independent experiments.

upregulation of 600% and 400% were detected at positions corresponding to 2 and 4 dyne/cm^2, respectively (Fig. 3b, c). With increasing SS, VCAM-1 and E-selectin decreased such that at 8 dyne/cm^2 expression was suppressed to a level below that induced by TNF-α stimulation under static conditions. These data indicate that SS has a potent and differential effect on expression of CAMs during inflammation.

Spatial mapping of shear-mediated CAM expression indicated that HAEC can regulate transcription and/or translation by sensing changes in SS on the order of 1 dyne/cm^2. In order to determine more precisely the spatial acuity of this inflammatory response, immunofluorescence of CAM expression was analyzed at a 10-fold higher spatial resolution along the shear gradient (Fig. 3d-f). Images were collected at 180 μm increments down the channel, corresponding to a 0.17 dyne/cm^2 decrease in SS over the area of HAEC analyzed. Analysis was focused on the regions of the flow channel, in which the greatest rate of change of CAM expression was observed in Fig. 3a–c. ICAM-1 expression measured over a range of 4–6.5 dyne/cm^2 revealed a linear increase at a rate of $\sim 25 \frac{\%}{\text{dyne/cm}^2}$ (Fig. 3d). By comparison, between 1.6–4 dyne/cm^2, VCAM-1 exhibited a much faster rate of decrease in expression $\sim 200 \frac{\%}{\text{dyne/cm}^2}$ (Fig. 3e). Between 7–9 dyne/cm^2, E-selectin decreased at a rate of $\sim 55 \frac{\%}{\text{dyne/cm}^2}$ (Fig. 3f). These data indicate that VCAM-1 expression is regulated with the highest spatial acuity in response to small fluctuations in SS. For instance, we measured a 50% drop in VCAM-1 expression over a distance of $\sim$300 μm down the channel, which corresponds to $\sim$10 EC responding to a decrease in SS of 0.25 dyne/cm^2.

To determine if HAEC would regulate CAM expression in a similar manner in a less steep SS gradient, we decreased the input volumetric flow rate by 30%. Thus, the maximum SS magnitude dropped from 16 to 11 dyne/cm^2 as defined by Equation 2, and the gradient was reduced from 0.82 to 0.57 dyne-cm^{-2}/mm. CAM expression over the shallower spatial gradient was measured and the relative change from static conditions were plotted in Fig. 4, at positions corresponding to the same SS as in Fig. 3 (a-c). Remarkably, no significant difference in shear-mediated CAM expression was observed. Thus, HAEC inflammatory response is more sensitive to changes in the magnitude of SS rather than the spatial variation with respect to regulation of CAM expression.

To elucidate the mechanism by which the CAM expression is upregulated in the case of ICAM-1, yet down-regulated for E-selectin and VCAM-1 with increased SS magnitude, we measured nuclear translocation and activation of NFκB, a promoter of many inflammatory genes [7]. The intensity of activated NFκB (phospho-p65) in the nucleus of individual HAEC as a function of SS down the channel was measured following 1 hour of 1 ng/mL TNF-α co-stimulation. We again employed antibody immunofluorescence to quantify HAEC activation expressed as the % of unstimulated static controls. As depicted in Fig. 5, the pattern of phospho-p65 nuclear translocation at 1 hour is similar to that of ICAM-1 upregulation detected at 4 hours. At SS above 9 dyne/cm^2, the percentage of activated HAEC is twice that of unstimulated static controls. Phospho-p65 translocation at SS below 6.5 dyne/cm^2 were not significantly different from HAEC stimulated with TNF-α under static conditions indicating that E-selectin and VCAM-1 upregulation at low SS does not correlate with the level of p65 activation at 1 hour of cytokine superposed with fluid shear.

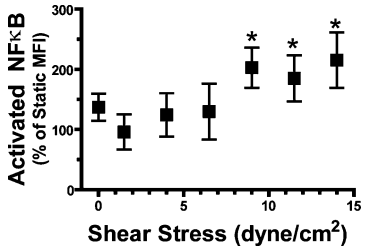

Figure 5. *TNF-α induced NFκB activation with shear stress in the Hele-Shaw chamber.* Nuclear translocation of phospho-p65 in HAEC after 1 hour of 1 ng/mL TNF-α treatment with concurrent shear stress was acquired by immunofluorescence microscopy. Data are presented as percentage of unstimulated static control EC MFI and shown as mean ± SEM from 4 independent experiments. *$p < 0.05$ versus 6.5, 4, 1.5, and 0 dyne/cm^2.

It is well established that monocytes are recruited to sites of atherosclerosis with much higher efficiency than neutrophils [24]. Monocytes are enriched at vascular sites of plaque formation, but the role of SS and differential regulation of CAM expression on recruitment efficiency remains obscure. Thus, we measured the multi-step process of leukocyte recruitment on HAEC that were stimulated with TNF-α and continuously exposed to a SS gradient in the same manner as described above. In order to assess leukocyte recruitment at a constant SS of 2 dyne/cm^2, a second flow chamber consisting of 3 independent rectangular flow channels was assembled to shear leukocytes perpendicularly across the HAEC monolayer (Fig. 6a). This facilitated imaging of leukocyte adhesion kinetics over regions pre-conditioned (i.e., differential CAM expression) at mean SS of 2, 6, and 12 dyne/cm^2, as well as the static condition. Adhesion dynamics were obtained from five random fields for each region of the channel allowing quantification of the number of leukocytes engaging in slow rolling, cell arrest, and transmigration to a position under the HAEC monolayers. Rolling monocytes were arrested with greater efficiency than rolling neutrophils for all regions. The recruitment efficiency, defined as the ratio of leukocyte arrest to those rolling, was ~1:1 for monocytes, whereas it was 1:3 for neutrophils over all regions, except at 12 dyne/cm^2 where rolling numbers decrease and arrest efficiency increased (Fig. 6b, c). Efficiency of recruitment for monocytes reached 85% within region I and only slightly declined within regions pre-sheared at higher magnitude (i.e., 80% at 6 dyne/cm^2 and 70% at 12 dyne/cm^2). In contrast, neutrophil recruitment efficiency was ~20%, even though rolling frequency was greatest within region I. Neutrophil adhesion efficiency reached ~66%

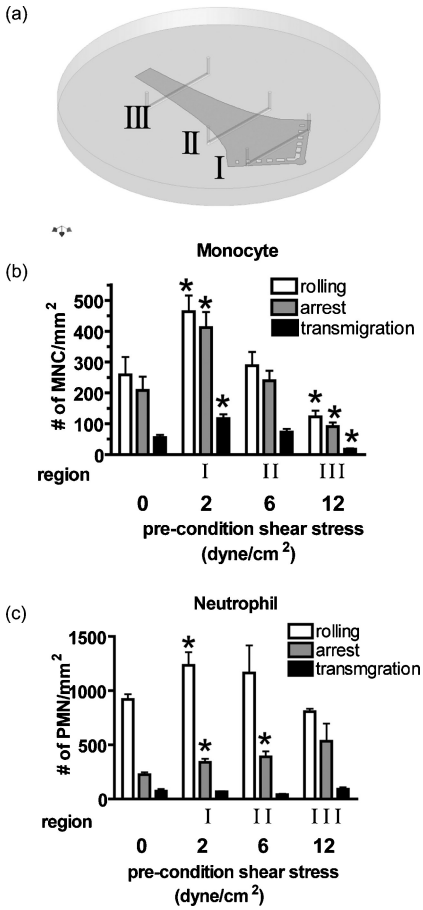

Figure 6. *Leukocyte recruitment on inflamed HAEC preconditioned over a linear gradient of shear stress.* (a) Leukocytes at 10^6/mL were perfused perpendicular to the direction that monolayers were pre-sheared at positions corresponding to 0, 2, 6 and 12 dyne/cm^2. The number of (b) monocytes (MNC) and (c) neutrophils (PMN) interacting with the endothelium were counted. Data are shown as mean ± SEM from 3 independent experiments. * $p < 0.05$ versus ECs in static condition.

within region III. These differences were observed despite the fact that the total number of neutrophils and monocytes interacting with the HAEC was similar within all regions preconditioned at different SS magnitudes. Interestingly, monocyte recruitment and transmigration was comparable on HAEC stimulated under static conditions or pre-sheared at 6 dyne/cm^2. In contrast, neutrophil recruitment efficiency increased at higher SS.

In a separate set of experiments, we examined monocyte recruitment flowing in a direction parallel to that of shear preconditioning, thereby, analyzing effects on EC in a geometry that more closely mimics leukocyte recruitment in the vasculature. As depicted in

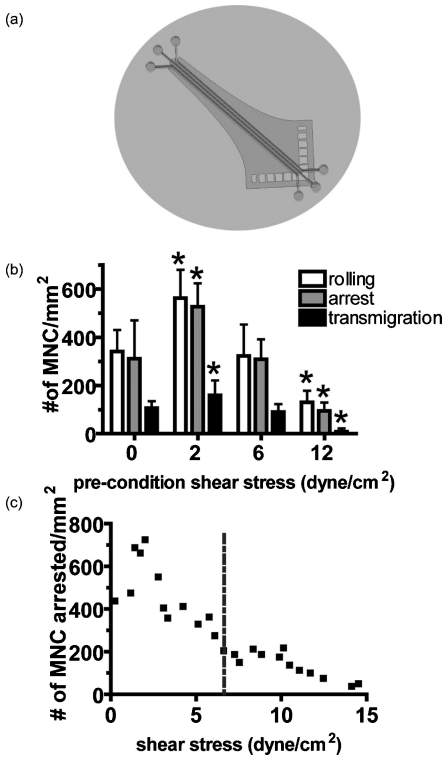

Figure 7. *Monocyte recruitment as a function of preconditioning shear stress.* (a) Monocytes (10^6/mL) were perfused at 2 dyne/cm^2 in the flow channels aligned parallel to the original flow direction on the EC monolayer. (b) The monocyte-endothelium interactions are plotted for specific pre-shearing magnitudes. Data are shown as mean ± SEM from 3 independent experiments. *$p<0.05$ versus ECs in static condition. (c) The number of monocytes firmly arrested along the rectangular channel as a function of preconditioning shear stress. Data is from one representative experiment.

Fig. 7a, the flow channels were aligned parallel to the direction of SS preconditioning in which HAEC were exposed to 0–16 dyne/cm^2 (Fig. 7a). Monocytes were again infused at a constant SS of 2 dyne/cm^2, and adhesive interactions over five fields were video recorded. Previous studies have shown that ECs start to elongate and align with the direction of laminar flow after only 3 hours of shear [22]; however, no difference in monocyte-EC interactions were detected for monocyte interaction with EC parallel to the direction of shear preconditioning (Fig. 7b). This suggests the initial modification in EC morphology or interactions along the gradient of CAM have minimum impact on monocyte recruitment.

A final analysis focused on how monocyte recruitment efficiency varies with position down the flow channel (Fig. 7c). This essentially provides a map of recruitment efficiency as a function of the differential expression of CAMs induced by cytokine and SS. A SS of ~7 dyne/cm^2 emerged as a critical value for altering CAM expression and favoring monocyte arrest, as recruitment efficiency increased significantly below this threshold. This observation is consistent with the fact that both E-selectin and VCAM-1 expression are elevated within this shear range. Significantly, E-selectin reached the greatest rate of change in expression between 6–9 dyne/cm^2. Thus, HAEC ligands that support monocyte capture and arrest are critical for optimum transition to stable adhesion and transmigration.

DISCUSSION

In arteries, maintenance of steady state SS within a narrow range (i.e., 15–20 dyne/cm^2) appears to be critical for maintaining vessel homeostasis. The anti-inflammatory action is attributed to mechanotransduction pathways that regulate the transcriptional response to cytokines. The focal nature of atherosclerosis associated with regions of low fluid shear and complex flow disturbances implies a central role for SS, and possibly the spatial heterogeneity of the shear field in EC dysfunction contributing to atherogenesis. In this study, we examined how EC spatially sense fluid SS and respond to inflammatory stimuli employing a custom fabricated microfluidic PPFC capable of exposing a HAEC monolayer to a linear gradient of SS. The linearity of the gradient and magnitude of SS at several locations within the flow chamber were characterized employing an ultrasonic flow imaging technique which reported a high degree of correlation ($R^2 = .99$) between measured and predicted SS. This model allowed us to discriminate between the effects of the magnitude and gradient of SS on EC inflammation. We discovered that regulation of CAM expression in the inflamed HAEC was most responsive to the magnitude of SS but insensitive to a 30% decrease in the spatial gradient of SS. The transition in shear-mediated CAM expression from atherogenic to atheroprotective (reflected by low E-selectin and VCAM-1 membrane expression) occurred within a narrow range of ~2–8 dyne/cm^2.

It was discovered that an incremental change in SS on the order of 0.25 dyne/cm^2 can be sensed by as few as ~10 EC to elicit a ~50% change in VCAM-1 expression. Nuclear translocation of phospho-p65 stimulated by TNF-α was a good predictor of the spatial regulation of ICAM-1 expression, increasing up

to a maximum at ~9 dyne/cm^2. Monocyte recruitment, a key step in atherogenesis, increased in direct proportion to the level of VCAM-1 and E-selectin but was independent of ICAM-1 expression. In contrast, the efficiency of neutrophil recruitment was severalfold less than that for monocytes, except within regions of high SS preconditioning where ICAM-1 expression was greatest. The implication is that these leukocyte subtypes are differentially recruited at vascular regions as a function of shear regulated CAM expression.

Mapping the response of TNF-α stimulated CAM expression as a function of the distance down the linear shear flow channel with high spatial resolution (~100 μm) revealed that each adhesion molecule exhibited a distinct expression pattern along the gradient of SS. Applying shear in the absence of cytokine exerted a subtle increase only in ICAM-1 expression and not the other CAMs. Our observations of cytokine-stimulated CAM expression in response to high fluid SS are consistent with that of Chiu [6] and Tsao [38], where attenuation in E-selectin and VCAM-1 expression was found after shearing the human umbilical vein endothelial cell monolayers at constant high shear (20 and 12 dyne/cm^2). The results for low-shear-mediated CAM expression also agree with the findings of Mohan et al. [26], where amplification in VCAM-1 expression was reported after shearing EC monolayer at low SS (2 dyne/cm^2). A similar upregulation pattern of ICAM-1 expression with an increase in SS was reported by Tsuboi et al. [40]. It is noteworthy that these studies were conducted at discrete magnitudes of SS over a range of 0–20 dyne/cm^2 using conventional PPFC delivering a uniform shear field [6, 26, 38, 40]. We present the first data of CAM expression mapped at the level of a single EC as a function of laminar SS on a single continuous endothelial monolayer using a microfluidic channel that accommodates a lower number of EC and smaller reagent volumes (~μL).

The greatest change in CAM expression on inflamed HAEC occurred within the low range in SS from 2–4 dyne/cm^2,correlating with SS values found within vascular regions prone to atherogenesis [25]. In contrast, TNF-α stimulated CAM expression was invariant at SS greater than 10 dyne/cm^2, which reflects the quiescence of inflammatory response within straight-unperturbed arterial regions (i.e., 12–17 dyne/cm^2). The rate of change of CAM expression was steepest between 2–8 dyne/cm^2, which suggests a mechanotransduction signaling pathway that modulates inflammation within this range of SS. Although the precise mechanisms by which SS superposes with cytokine to regulate inflammatory gene expression have yet to be determined, it is clear that they act through distinct, often converging pathways to modulate the activity of transcription factors associated with inflammation including NFκB, AP-1, GATA, specificity protein-1 (SP-1), and IFN regulatory factor-1 (IRF-1) [9, 21, 27, 29, 42, 44]. Activation of these factors and their binding to distinct promoter regions result in the induction and in some cases the suppression of inflammatory genes.

NFκB (p65/p50 heterodimer) is known to bind the first identified cis-acting *shear stress responsive element* and mediates expression of many cytokine induced genes active during vascular inflammation and atherogenesis [7, 16, 18]. The pattern of phospho-p65 translocation most closely matched upregulation of ICAM-1, since both increased along the SS gradient. This pattern of regulation may be expected as the ICAM-1 gene has functional binding sites for NFκB [21, 44]. Remarkably, phospho-p65 levels were not elevated at lower SS (i.e., 1.5–4 dyne/cm^2) compared to static control even though this was the region over which VCAM-1 and E-selectin upregulation was greatest. This was surprising since both VCAM-1 and E-selectin promoters contain binding sites for NFκB [17, 27, 29, 35]. However, this observation is congruent with Yamawaki et al., who reported that SS mediated down regulation of VCAM-1 expression did not correspond with changes in NFκB activity, but instead correlated with down regulation of JNK and p38 MAP Kinases [46]. One possibility is that NFκB dependent VCAM-1 and E-selectin expression occur over different time scales than ICAM-1 expression. What is more probable is that NFκB plays a role in expression of all three CAMs, but control of ICAM-1 transcription is most sensitive to NFκB activation. This notion is supported by a study showing that over-expression of p65 in HUVEC transactivated an NFκB binding site within the promoter region of ICAM-1 [21].

Additional insight into the mechanisms by which inflammatory CAM expression are regulated by distinct transcriptional programs is found in a recent report showing that phenyl methimazole dramatically inhibits TNF-α induced VCAM-1 expression[9]. However, this inhibitor exerted a modest effect on E-selectin upregulation and no effect on ICAM-1 expression on HAEC. The mechanism involved reduction in IRF-1 binding activity to the VCAM-1 promoter. Relevant to the current studies is the finding that phenyl methimazole also significantly

reduced TNF-α activated monocytic cell adhesion to HAEC under shear flow conditions. This is in agreement with our data which revealed a decrease in TNF-α induced monocyte recruitment on monolayers conditioned at high SS where VCAM-1 expression was decreased.

In addition to IRF-1 and NFκB, the VCAM-1 promoter contains binding sites for AP-1, SP-1, and GATA [17, 27 – 29], while E-selectin contains binding sites for NFκB and HOXA9 [3, 35]. Shear stress has been shown to increase AP-1 binding activity and is involved in the negative transcriptional regulation of the VCAM-1 gene, perhaps through an upstream silencer on the promoter [19, 20]. Furthermore, HOXA9 expression in EC has been shown to be dependent on the magnitude and duration of SS [32]. A simple mechanistic view for the differential CAM regulation we observed is that SS differentially activates NFκB, as well as other factors such as HOXA9, AP-1, IRF-1, and MAP kinases. We hypothesize that within regions of relatively high SS ($\geq$8 dyne/cm^2), in the presence of TNF-α stimulation, HOXA9 and IRF-1 have less transcriptional activity on the promoters of E-selectin and VCAM-1, whereas ICAM-1 is acutely promoted by activation of NFκB and less sensitive to the inhibitory effect of these factors.

Inflamed HAEC stimulated with TNF-α and exposed to low SS were more effective at recruiting monocytes, than neutrophils. Gonzales et al.[15] reported a similar result for EC preconditioned at 2 dyne/cm^2 where monocyte adhesion increased 3-fold above static culture [15]. Our data are the first to show that neutrophils are preferentially recruited within regions of inflamed HAEC pre-exposed to a high SS of 12 dyne/cm^2. Leukocyte adhesive interactions are dependent on the relative level of CAMs expressed on the EC membrane and the corresponding integrins and selectin receptors on the leukocytes [37]. LFA-1, VLA-4, and PSGL-1 expressed on monocytes are known to recognize ICAM-1, VCAM-1, and E-selectin, respectively, on the HAEC surface. E-selectin is required for cell tethering and rolling, whereas ICAM-1 and VCAM-1 are receptors that mediate leukocyte arrest and transmigration [11]. The efficiency of monocyte arrest correlated directly with VCAM-1 but not ICAM-1 expression, implying that VCAM-1 is the primary ligand mediating arrest. On the other hand, neutrophils predominantly express LFA-1, which binds with high affinity to ICAM-1. This was consistent with the observation that the efficiency of neutrophil recruitment was positively correlated to ICAM-1 expression pattern. The efficiency of capture and rolling for monocytes and neutrophils were both closely correlated to the expression pattern of E-selectin. Our findings that monocyte recruitment efficiency varied directly with shear-regulated VCAM-1 expression may explain VCAM-1's central role in atherogenesis [8] and why recruitment of monocytes occurs preferentially over neutrophils [24]. The high sensitivity of VCAM-1 expression to small perturbations in SS over small distances ($\sim$170 μm) also underscores the focal nature of atherosclerosis in which plaque formation maps to regions of low SS [13].

In evaluating our results, we considered the possibility that HAEC in regions of low shear downstream of HAEC exposed to high SS may be influenced via paracrine signaling to induce an anti-inflammatory phenotype. However, the magnitude of the changes induced by SS compared to cytokine treatment alone in the downstream region of the chamber coupled with the dramatic drop in VCAM-1 expression over a very small distance led us to conclude that any response to paracrine signaling was small compared to cytokine and mechano-signaling in our chamber and did not play a significant role in the observed responses.

Intercellular communication through gap and adherens junctions is another means by which a neighboring EC may influence responses to shear flow. For example, De Paola et al. [12] reported that EC exposed to flow separation and recirculation upregulated gap junction protein connexin 43 (Cx43) transcripts and led to disorganization of Cx43 protein resulting in impaired communication [12]. Intercellular communication through adherens junctions containing PECAM-1, VE-Cadherin, and VEFR2 has also been reported for ECs under SS. These junctional proteins are known to activate cytoskeletal remodeling, WOW-1 binding, NFκB, AKT, PI(3)K, and Src in monolayers exposed to constant SS [41].

We also considered the possibility that injury or damage to EC brought about by the placement of the second chamber over the pre-sheared monolayer would release soluble mediators affecting subsequent inflammatory responses. Although we would expect such mediators to equally affect EC across the monolayer, notably, we have yet to observe any markers of EC inflammation following placement of the flow chamber in the absence of cytokine.

A significant finding is that CAM expression is dominated by the absolute magnitude of SS rather than the spatial gradients in the unidirectional laminar

SS. However, one must consider that this relationship might be different *in vivo* where shear gradients can be greater [12], and there is the potential for more complex cellular interactions, such as influence from intima and smooth muscle cells [5]. Although the design of the flow chamber allowed us to map the endothelial response over regions of well defined gradients, we note that one limitation of the Hele-Shaw channel is that we cannot independently vary at any position both the SS magnitude and its gradient. Nonetheless, others have also observed that the spatial gradient in SS is not a predominant factor in EC proliferation, despite the fact that a different flow profile was applied [45]. Additionally, monocyte recruitment data reported by Chen et al. [4]support the concept that the spatial shear gradient is not the primary factor affecting monocyte arrest on the endothelium.

In summary, we present the first study which maps CAM regulation, NFκB activation and leukocyte recruitment as a function of unidirectional laminar SS over a spatial gradient. The data show that EC can sense changes on the order of 0.25 dyne/cm^2, and this has a direct influence on protein transcription and CAM expression during inflammation. VCAM-1 expression most closely correlated with the efficiency of monocyte recruitment, which increased markedly on HAEC pretreated below a threshold level of $\sim$7 dyne/cm^2. We conclude that the magnitude of shear force as sensed by endothelium within vascular regions of disturbed blood flow is a critical determinant in the spatial regulation of the inflammatory response and atherogenesis.

REFERENCES

1. Abbot SE, Whish WJD, Jennison C, Blake DR, Stevens CR. (1999). Tumour necrosis factor alpha stimulated rheumatoid synovial microvascular endothelial cells exhibit increased shear rate dependent leucocyte adhesion in vitro. *Ann Rheum Dis* 58:573–581.
2. Aird WC. (2006). Mechanisms of endothelial cell heterogeneity in health and disease. *Circ Res* 98:200–208.
3. Bandyopadhyay S, Ashraf MZ, Daher P, Howe PH, DiCorleto PE. (2007). HOXA9 participates in the transcriptional activation of E-selectin in endothelial cells. *Mol Cell Biol* 27:4207–4216.
4. Chen CN, Chang SF, Lee PL, Chang K, Chen LJ, Usami S, Chien S, Chiu JJ. (2006). Neutrophils, lymphocytes, and monocytes exhibit diverse behaviors in transendothelial and subendothelial migrations under co-culture with smooth muscle cells in disturbed flow. *Blood* 107:1933–1942.
5. Chiu JJ, Chen LJ, Lee PL, Lee CI, Lo LW, Usami S, Chien S. (2003). Shear stress inhibits adhesion molecule expression in vascular endothelial cells induced by coculture with smooth muscle cells. *Blood* 101:2667–2674.
6. Chiu JJ, Lee PL, Chen CN, Lee CI, Chang SF, Chen LJ, Lien SC, Kao YC, Usami S, Chien S. (2004). Shear stress increases ICAM-1 and decreases VCAM-1 and E-selectin expressions induced by tumor necrosis factor-α in endothelial cells. *Arterioscler Thromb Vasc Biol* 24:73–79.
7. Collins T, Cybulsky MI. (2001). NF-kappaB: pivotal mediator or innocent bystander in atherogenesis? *J Clin Invest* 107:255–264.
8. Cybulsky MI, Iiyama K, Li H, Zhu S, Chen M, Iiyama M, Davis V, Gutierrez-ramos JC, Connelly PW, Milstone DS. (2001). A major role for VCAM-1, but not ICAM-1, in early atherosclerosis. *J Clin Invest* 107:1255–1262.
9. Dagia NM, Harii N, Meli AE, Sun X, Lewis CJ, Kohn LD, Goetz DJ. (2004). Phenyl methimazole inhibits TNF-alpha-induced VCAM-1 expression in an IFN regulatory factor-1-dependent manner and reduces monocytic cell adhesion to endothelial cells. *J Immunol* 173:2041–2049.
10. Dardik A, Chen LL, Frattini J, Asada H, Aziz F, Kudo FA, Sumpio BE. (2005). Differential effects of orbital and laminar shear stress on endothelial cells. *J Vasc Surg* 41:869–880.
11. Dejana E, Breviario F, Caveda L. (1994). Leukocyte-endothelial cell adhesive receptors. *Clin Exp Rheumatol* S10:25–28.
12. DePaola N, Gimbrone MA, Davies PF, Dewey F. (1992). Vascular endothelium responds to fluid shear stress gradients. *Arterioscler Thromb* 12:1254–1257.
13. Giddens DP, Zarins ZK, Glagov S. (1993). The role of fluid mechanics in the localization and detection of atherosclerosis. *J Biomech Eng* 115:588–594.
14. Goldsmith HL, Quinn TA, Drury G, Spanos C, McIntosh FA, Simon SI. (2001). Dynamics of neutrophil aggregation in couette flow revealed by videomicroscopy: effect of shear rate on two-body collision efficiency and doublet lifetime. *Biophys J* 81:2020–2034.
15. Gonzales RS, Wick TM. (1996). Hemodynamic modulation of monocytic cell adherence to vascular endothelium. *Annals of Biomedical Engineering* 24:382–393.
16. Hajra L, Evans AI, Chen M, Hyduk SJ, Collins T, Cybulsky MI. (2000). The NF-kappa B signal transduction pathway in aortic endothelial cells is primed for activation in regions predisposed to atherosclerotic lesion formation. *Proc Natl Acad Sci U S A* 97:9052–9057.
17. Iademarco MF, McQuillan JJ, Rosen GD, Dean DC. (1992). Characterization of the promoter for vascular cell adhesion molecule-1 (VCAM-1). *J Biol Chem* 267:16323–16329.

18. Khachigian LM, Resnick N, Gimbrone MA, Jr., Collins T. (1995). Nuclear factor-kappa B interacts functionally with the platelet-derived growth factor B-chain shear-stress response element in vascular endothelial cells exposed to fluid shear stress. *J Clin Invest* 96:1169–1175.
19. Korenaga R, Ando J, Kosaki K, Isshiki M, Takada Y, Kamiya A. (1997). Negative transcriptional regulation of the VCAM-1 gene by fluid shear stress in murine endothelial cells. *Am J Physiol* 273:C1506–1515.
20. Lan Q, Mercurius KO, Davies PF. (1994). Stimulation of transcription factors NF kappa B and AP1 in endothelial cells subjected to shear stress. *Biochem Biophys Res Commun* 201:950–956.
21. Ledebur HC, Parks TP. (1995). Transcriptional regulation of the intercellular adhesion molecule-1 gene by inflammatory cytokines in human endothelial cells. Essential roles of a variant NF-kappa B site and p65 homodimers. *J Biol Chem* 270:933–943.
22. Li YSJ, Haga JH, Chien S. (2005). Molecular basis of the effects of shear stress on vascular endothelial cells. *J Biomech* 38:1949–1971.
23. Libby P. (2002). Inflammation in atherosclerosis. *Nature* 420:868–874.
24. Lusis AJ. (2000). Atherosclerosis. *Nature* 407:233–241.
25. Malek AM, Alper SL, Izumo S. (1999). Hemodynamic shear stress and its role in atherosclerosis. *JAMA* 282:2035–2042.
26. Mohan S, Mohan N, Valente AJ, Sprague EA. (1999). Regulation of low shear flow-induced HAEC VCAM-1 expression and monocyte adhesion. *Am J Physiol* 276:C1100–C1107.
27. Neish AS, Williams AJ, Palmer HJ, Whitley MZ, Collins T. (1992). Functional analysis of the human vascular cell adhesion molecule 1 promoter. *J Exp Med* 176:1583–1593.
28. Neish AS, Khachigian LM, Park A, Baichwal VR, Collins T. (1995). Sp1 is a component of the cytokine-inducible enhancer in the promoter of vascular cell adhesion molecule-1. *J Biol Chem* 270:28903–28909.
29. Neish AS, Read MA, Thanos D, Pine R, Maniatis T, Collins T. (1995). Endothelial interferon regulatory factor 1 cooperates with NF-kappa B as a transcriptional activator of vascular cell adhesion molecule 1. *Mol Cell Biol* 15:2558–2569.
30. Passerini AG, Polacek DC, Shi C, Francesco NM, Manduchi E, Grant GR, Pritchard WF, Powell S, Chang GY, Stoeckert CJ Jr, Davies PF. (2004). Coexisting proinflammatory and antioxdative endothelial transcription profiles in a distubed flow region of the adult porcine aorta. *Proc Natl Acad Sci USA* 101:2482–2487.
31. Ross R. (1993). The pathogenesis of atherosclerosis: a perspective for the 1990s. *Nature* 362:801–809.
32. Rossig L, Urbich C, Bruhl T, Dernbach E, Heeschen C, Chavakis E, Sasaki K, Aicher D, Diehl F, Seeger F, Potente M, Aicher A, Zanetta L, Dejana E, Zeiher AM, Dimmeler S. (2005). Histone deacetylase activity is essential for the expression of HoxA9 and for endothelial commitment of progenitor cells. *J Exp Med* 201:1825–1835.
33. Samijo SK, Willigers JM , Brands PJ, Barkhuysen R, Reneman RS, Kitslaar PJ, Hoeks APG. (1997). Reproducibility of shear rate and shear stress assessment by means of ultrasound in the common carotid artery of young human males and females. *Ultrasound in Med & Biol* 23:583–590.
34. Schaff UY, Xing MM, Lin KK, Pan N, Jeon NL, Simon SI. (2007). Vascular mimetics based on microfluidics for imaging the leukocyte–endothelial inflammatory response. *Lab Chip* 7:448–456.
35. Schindler U, Baichwal VR. (1994). Three NF-kappa B binding sites in the human E-selectin gene required for maximal tumor necrosis factor alpha-induced expression. *Mol Cell Biol* 14:5820–5831.
36. Sheikh S, Rahman M, Gale Z, Luu NT, Stone PCW, Matharu NM, Rainger GE, Nash GB. (2005). Differing mechanisms of leukocyte recruitment and sensitivity to conditioning by shear stress for endothelial cells treated with tumour necrosis factor-α or interleukin-1β. *Br J Pharmacol* 145:1052–1061.
37. Simon SI, Green CE. (2005). Molecular mechanics and dynamics of leukocyte recruitment during inflammation. *Annu Rev Biomed Eng* 7:151–185.
38. Tsao PS, Buitrago R, Chan JR, Cooke JP. (1996). Fluid flow inhibits endothelial adhesiveness. *Circulation* 94:1682–1689.
39. Tsou JK, Liu J, Insana MF. (2006). Modeling and phantom studies of ultrasonic wall shear rate measurements using coded pulse excitation. *IEEE Trans Ultrason Ferroelec Freq Contrl* 53:724–734.
40. Tsuboi H, Ando J, Korenaga R, Takada Y, Kamiya A. (1995). Flow stimulates ICAM-1 expression time and shear stress dependently in cultured human endothelial cells. *Biochemical and Biophysical research communications* 206:988–996.
41. Tzima E, Irani-Tehrani M, Kiosses WB, Dejana E, Schultz DA, Engelhardt B, Cao G, DeLisser H, Schwartz MA. (2005). A mechanosensory complex that mediates the endothelial cell response to fluid shear stress. *Nature* 437:426–431.
42. Umetani M, Mataki C, Minegishi N, Yamamoto M, Hamakubo T, Kodama T. (2001). Function of GATA transcription factors in induction of endothelial vascular cell adhesion molecule-1 by tumor necrosis factor-alpha. *Arterioscler Thromb Vasc Biol* 21:917–922.
43. Usami S, Chen HH, Zhao Y, Chien S, Skalak R. (1993). Design and construction of a linear shear stress flow chamber. *Annals of Biomedical Engineering* 21:77–83.

44. Voraberger G, Schafer R, Stratowa C. (1991). Cloning of the human gene for intercellular adhesion molecule 1 and analysis of its 5'-regulatory region. Induction by cytokines and phorbol ester. *J Immunol* 147:2777–2786.
45. White CR, Haidekker M, Bao X, Frangos JA. (2001). Temporal gradients in shear, but not spatial gradients, stimulate endothelial cell proliferation. *Circulation* 103:2508–2513.
46. Yamawaki H, Lehoux S, Berk BC. (2003). Chronic Physiological Shear Stress Inhibits Tumor Necrosis Factor-Induced Proinflammatory Responses in Rabbit Aorta Perfused Ex Vivo. *Circulation* 108:1619–1625.
47. Young RE, TR, Nourshargh S. (2002). Divergent mechanisms of action of the inflammatory cytokines interleukin 1-beta and tumour necrosis factor- alpha in mouse cremasteric venules. *Br J Pharmacol* 137:1237–1246.